Microchim Acta (2013) 180:581–587
DOI 10.1007/s00604-013-0960-4

ORIGINAL PAPER

A study on the direct electrochemistry and electrocatalysis of microperoxidase-11 immobilized on a porous network-like gold film: Sensing of hydrogen peroxide

Qian-Li Zhang · Ai-Jun Wang · Zi-Yan Meng · Ya-Hui Lu · Hong-Jun Lin · Jiu-Ju Feng

Received: 13 December 2012 / Accepted: 2 February 2013 / Published online: 21 February 2013

Abstract We have prepared porous and network-like nanofilms of gold by galvanic replacement of a layer of copper particles acting as a template. The films were first characterized by scanning electron microscopy and X-ray diffraction, and then modified with cysteamine so to enable the covalent immobilization of the enzyme microperoxidase-11. The immobilized enzyme undergoes direct electron transfer to the underlying electrodes, and the electrode displays high electrocatalytic activity towards the reduction of oxygen and hydrogen peroxide, respectively, owing to the largely enhanced electroactive surface of the porous gold film. The detection limit of H_2O_2 is 0.4 μM (3 S/N).

Keywords Electrodeposition · Porous network-like Au film · Microperoxidase-11 · Electrocatalysis

Electronic supplementary material The online version of this article (doi:10.1007/s00604-013-0960-4) contains supplementary material, which is available to authorized users.

Q.-L. Zhang · A.-J. Wang · Z.-Y. Meng · H.-J. Lin · J.-J. Feng (✉)
College of Chemistry and Life Science, College of Geography and Environmental Science, Zhejiang Normal University, Jinhua 321004, China
e-mail: jjfengnju@gmail.com

Q.-L. Zhang
School of Chemistry and Biological Engineering, Suzhou University of Science and Technology, Suzhou 215009, China

Y.-H. Lu
School of Chemistry and Chemical Engineering, Henan Normal University, Xinxiang 453007, China

Introduction

Microperoxidase-11 (MP-11) was obtained from enzymatic cleavage of horse heart cytochrome c [1]. It contains a heme group linked with a helical chain via two thioether bonds of cysteine residues, in addition to one of the axial coordination sites of iron (III) occupied by a histidine residue [2]. Because of smaller size and relative simplicity, MP-11 is usually used as a benchmark model system to imitate the behavior of macrobiomolecules such as hemoproteins and some enzymes [3, 4]. Meanwhile, it is easy to achieve the direct electron transfer of the immobilized MP-11 with the electrodes. Thus, MP-11 is widely used for the construction of third-generation biosensors in the detection of some small molecules such as hydrogen peroxide (H_2O_2) [5, 6] and nitric oxide [7, 8]. Furthermore, these works can be extended to biofuel cells, where the MP-11 modified electrodes are usually used as cathode materials for electrocatalytic reduction of oxygen (O_2) [9–11].

For the fabrication of the third-generation electrochemical biosensors, the pre-requirement is the achievement of direct electron transfer of the immobilized protein with underlying electrode. Conventionally, this target is always difficult when MP-11 is directly immobilized on the bare electrode. Now, it is possible using the promoters modified electrode to provide a biocompatible microenvironment [4, 12].

Au nanoparticles have been demonstrated an efficient platform for immobilizing protein, because of their good biocompatibility, conductivity, and mechanical stability [13–15]. Recently, synthesis of Au films with different shapes has received great success [16–18], especially for

the porous Au films. The porous Au films are expected to increase the protein load, and hence have the ability to improve the sensitivity of the biosensors. Moreover, Au nanoparticles in the porous walls can act as a electron relay center to facilitate the electron transfer between the immobilized protein and underlying electrode [19].

In general, dealloying and templating are usually used for the construction of porous Au films [5, 20, 21]. For the former, binary gold alloys are firstly constructed, where the less noble elements are selectively removed by chemical or electrochemical corrosion [22]. In the case of templating, different sized templates are firstly deposited on the substrates. Then, the porous Au films are obtained through the deposition of Au nanoparticles, followed by the removal of the templates [3, 10].

In this work, a simple method was developed to prepare porous network-like Au film, using the electrodeposited Cu film on a glass carbon electrode as a template. The as-prepared Au film was covered by a layer of cysteamine by self-assembly for biocompatible and covalent immobilization of MP-11, which remained native electrochemical activity and showed good performance towards the reduction of O_2 and H_2O_2, respectively.

Experimental section

Materials

MP-11, $HAuCl_4$, $CuCl_2$, H_2O_2 solution (30 %), cysteamine, 1-ethyl-3-(3- dimethylaminopropyl) carbodiimide (EDC), and ethylenediamine (EDA) were purchased from Shanghai Chemical Reagent Works (Shanghai, China) and used as received. Other reagents were of analytical grade and used without further purification. All aqueous solutions were prepared with twice-distilled water.

Electrodeposition of the Cu films as templates

A glassy carbon electrode (GCE, d=3 mm) was used as the working electrode for electrodeposition of Cu film. Firstly, the electrode was polished with 1.0, 0.3, and 0.05 μm Al_2O_3 slurry, and successively ultrasonicated in water and ethanol for 5 min, respectively. The electrode was dried with N_2 stream at room temperature.

For the construction of Cu film, a clean GCE was put into 50 mM $CuCl_2$ solution containing 50 mM EDA (pH7.0, adjusted with dilute ammonia solution), and applied a constant potential of −0.65 V for 5 min. Afterwards, the electrode was washed with water and dried with N_2 stream at room temperature (denoted as Cu/GCE).

Construction of porous network-like Au films

For the construction of porous network-like Au films, the Cu/GCE was immersed into 5 mM $HAuCl_4$ for 15 min, the Au nanoparticles was obtained via galvanic replacement. The resultant electrode is abbreviated as Cu@Au/GCE. Then, the electrode was placed into 2 M HNO_3 solution for 10 h to remove the un-reacted Cu templates. Next, the porous network-like Au film modified electrode was placed in 0.5 MH_2SO_4 solution and cyclic scanning until only the characteristic peaks of Au are detected in the cyclic voltammograms (CVs). The porous network-like Au film modified electrode (denoted as Au/GCE) was thoroughly washed with water and dried with N_2 stream.

Construction of the MP-11 biosensor

In general, cysteamine molecules are self-assembled onto Au surface due to the formation of S-Au bond. Conversely, the –COOH groups in cysteamine molecules can covalently link to the $–NH_2$ of lysine residues surrounding the partially exposed heme center in MP-11, with the assistance of EDC. Specifically, the Au/GCE was firstly dipped into a 50 mM cysteamine solution for 10 h to form stable self-assembled monolayers (denoted as the cysteamine/Au/GCE) for biocompatible immobilization of the protein. Then, the cysteamine/Au/GCE was immersed into an EDC solution (1 mg · mL^{-1}) for 60 min to active the –COOH groups in cysteamine. Afterwards, the activated cysteamine/Au/GCE was put into a MP-11 solution (0.8 mg·mL^{-1}, prepared with 10 mM phosphate solution) for 24 h at 4 °C. The resultant electrode is named as MP-11/cysteamine/Au/GCE and stored in 10 mM phosphate solution at 4 °C when not in use. The detail preparation process is described in Scheme 1.

Similarly, the MP-11/cysteamine/Cu@Au/GCE and MP-11/cysteamine/Cu/GCE were also prepared under the same conditions, without removing the Cu templates or the deposition of Au films.

Instruments

Electrochemical experiments were performed using a CHI 660D electrochemical workstation (Shanghai Chenhua, China, Co., Ltd., China, www.chi.instrument.com.cn). A platinum wire and a saturated calomel electrode (SCE) were used as counter and reference electrodes, respectively. The bare or modified GCE was used as working electrodes. All experiments were carried out at room temperature. The morphologies and dimensions of the samples were characterized by scanning electron microscopy (SEM, JSM-6390LV microscope, JEOL, Japan, www.jeol.cn). The X-

Scheme 1 Scheme for the construction of the MP-11/cysteamine/Au/GCE

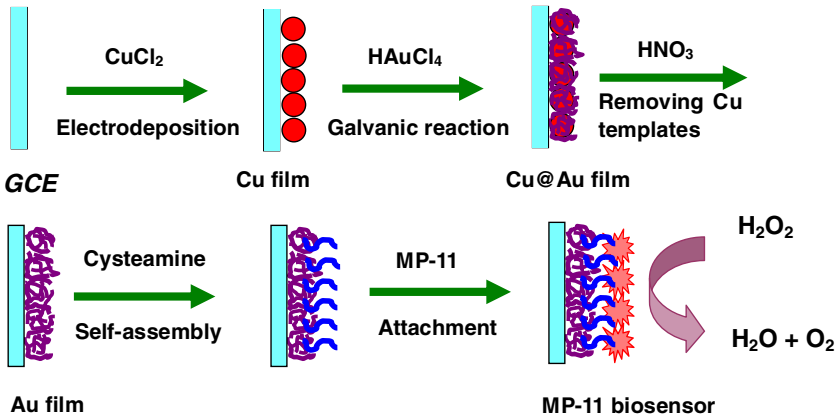

ray diffraction (XRD, Rigaku Dmax-2000 diffractometer, USA, www.rigaku.com) analysis was carried out with a Cu Kα radiation source.

Results and discussion

Morphological and structural characterization

Figure 1a shows the SEM image of the Cu deposits by applying a constant potential of −0.65 V in a 50 mM $CuCl_2$ solution containing 50 mM EDA for 5 min. Notably, the Cu deposits include a variety of smooth spherical Cu particles about 270±10 nm. Using the as-prepared Cu film as a sacrificial template, the porous network-like Au film was prepared through simple galvanic replacement for 15 min, followed by the removal of the template in 2 M HNO_3 solution (Fig. 1b-c). The thickness of the Au film is about 300–350 nm, which strongly depends on the particles size of the Cu film. The porous inter-connected walls are aggregated by many small Au particles, cross-link together, and finally form the coral-like Au nanostructures.

The XRD results confirm the formation of the Cu film (Fig. 2a, curve b) and the porous network-like Au film (Fig. 2a, curve c). For the former, the peak at 43.6° is assigned to the (111) crystal planes of Cu, and the peak at 28.6° is attributed to the emergence of Cu_2O for the oxidation of Cu itself in air [23]. In curve c, the XRD pattern of the porous network-like Au film gives further support to the quality and purity of Au, showing the characteristic peaks at 38.2°, 44.3°, 64.4°, and 72.6°, which are assigned to the (111), (200), (220), and (311) crystal planes of Au, respectively. These values are in good agreement with the face-centered cubic (fcc) structure of Au [24, 25]. Moreover, the disappearance of the typical peak from Cu proves the completely removal of Cu from the Au lattice. For comparison, the XRD pattern of the bare GCE is also presented (Fig. 2a, curve a).

Additionally, as displayed in Fig. S1 (Supporting Information), the electrochemical characterization of the

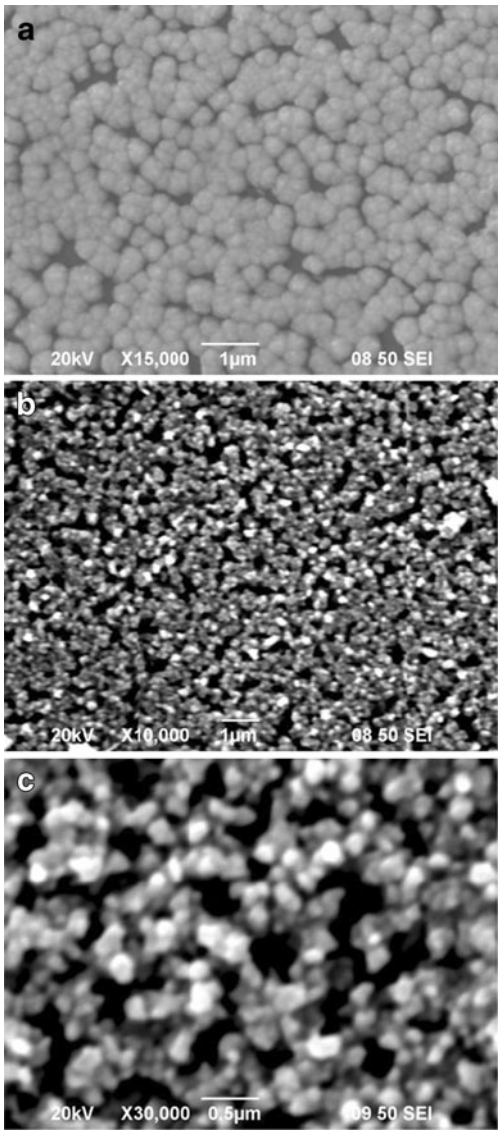

Fig. 1 SEM images of the Cu (**a**) and porous network-like Au (**b**) films, and high magnification of Au films (**c**)

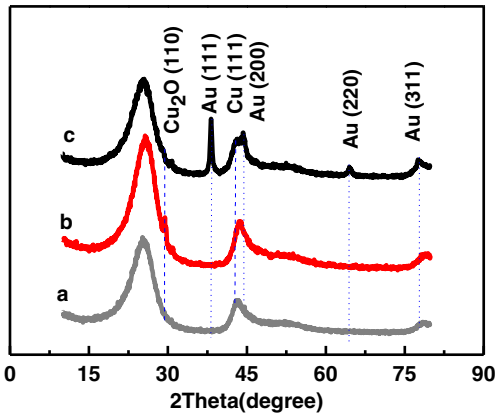

Fig. 2 XRD patters of the bare (curve **a**), Cu (curve **b**), and porous network-like Au (curve **c**) films modified GCE

Au/GCE also confirm high quality of the porous network-like Au film [26]. Meanwhile, with integration of the reduction peak, the electroactive surface area of the Au/GCE was determined to be 1.13 cm^2 by assuming that the reduction of a monolayer of gold oxide requires 386 $\mu C \cdot cm^{-2}$. This value is larger than that of three-dimensionally ordered macroporous Au structures with a value of 0.956 cm^2 [27] and Au dendrites with a value of 0.153 cm^2 [26].

Direct electron transfer of MP-11

Cyclic voltammetry is a useful tool to examine the bioactivity of the electroactive species on electrode surface, such as the immobilized MP-11 as a model probe in our system. Figure 3 shows a couple of stable and well-defined peaks on the MP-11/cysteamine/Au/GCE in a phosphate solution (pH7.0) with different scan rates. Obviously, the responses of the modified electrodes were attributed to the redox of the electroactive center of the immobilized protein.

Specifically, when MP-11 was immobilized on the cysteamine/Au/GCE, the oxidation and reduction peaks are located at −0.35 V and −0.40 V, and the separation between them is about 50 mV with nearly equal redox peak currents (Fig. 3). It indicates that the immobilized MP-11 undergoes a nearly reversible electrochemical process. The formal potential ($E^{0'}=(E_{pa}+E_{pc})/2$) of the protein is ca. –0.38 V, similar to that of MP-11 (−0.38 V) dispersed in phosphate solution [4]. Meanwhile, the anodic and cathodic peak currents of the immobilized protein linearly increase in the scan rate range from 10 to 100 $mV \cdot s^{-1}$ with correlation coefficients of 0.999 (Fig. 3b), while the separation of the redox peak potentials are almost unchanged (data not shown). These results suggest that the redox reaction of the immobilized MP-11 is a surface-controlled process [28].

The redox peak currents (I_p) of the immobilized MP-11 increase with scan rates following the equation [28, 29]:

$$I_p = \frac{n^2F^2Av\Gamma}{4RT}$$

where I_p represents the anodic or cathodic peak currents, A is the real surface area of the porous network-like Au film modified electrode, and Γ is the surface coverage of the electroactive MP-11 on the cysteamine/Au/GCE. In our work, the Γ is calculated to be about 3.26×10^{-10} $mol \cdot cm^{-2}$, which is larger than that of MP-11 on the cysteamine/Cu@Au/GCE (2.17×10^{-10} $mol \cdot cm^{-2}$), but smaller than that of MP-11 on the chitosan-graphene nanocomposite (4.71×10^{-10} $mol \cdot cm^{-2}$) [4].

The electron transfer rate constant (k_s) of the immobilized MP-11 was obtained based on Laviron's equation [30]:

$$K_s = \frac{nFv}{m^{-1}RT}$$

where m is a parameter related to the peak-to-peak separation potential, R, T, and F have their conventional meanings. The value of k_s is around 2.27 s^{-1} at 70 $mV \cdot s^{-1}$ on the MP-11/cysteamine/Au/GCE. These results further support our assumption that the porous network-like Au film is an excellent promoter for the direct electron transfer of MP-11 with the electrodes.

For comparison, control experiments were carried out as MP-11 covalently immobilized on the cysteamine/Cu@Au/GCE

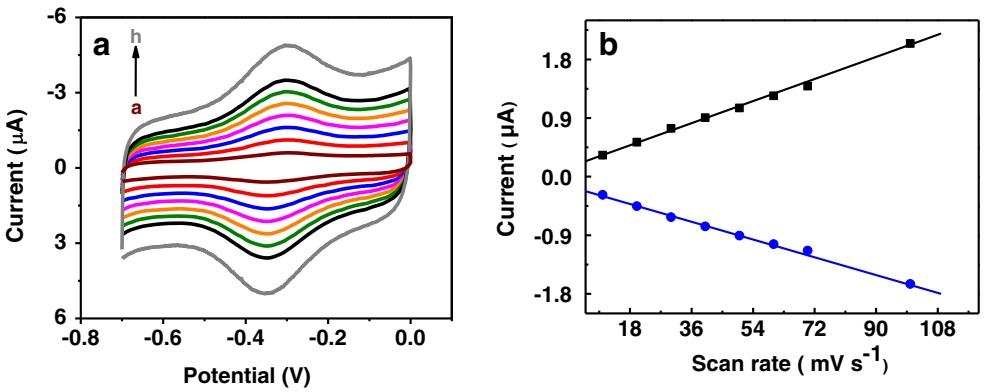

Fig. 3 **a** CVs of the MP-11/cysteamine/Au/GCE with different scan rates (curve a–h) in 20 mM phosphate solution (pH 7.0): 10, 20, 30, 40, 50, 60, 70, and 100 $mV \cdot s^{-1}$. **b** The oxidation and reduction currents *vs*. scan rates

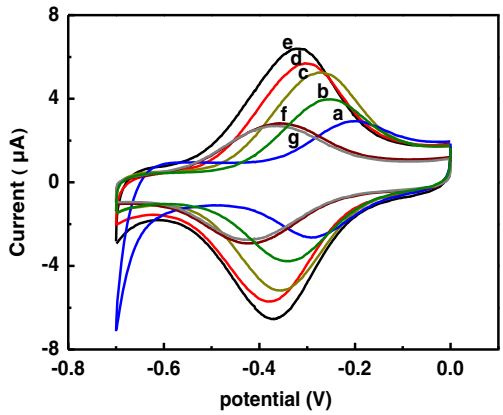

Fig. 4 CVs of the MP-11/cysteamine/Au/GCE with different pH (a–g) in 20 mM phosphate solution at 50 mV · s^{-1}: 3.0, 4.0, 5.0, 6.0, 7.0, 8.0, and 9.0

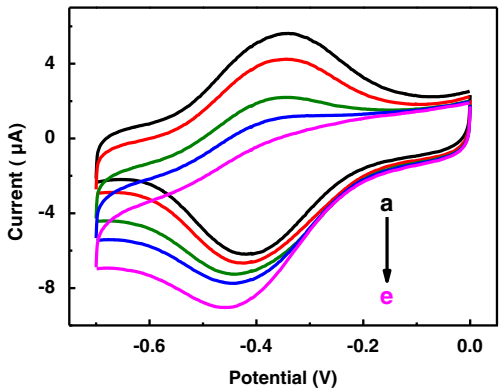

Fig. 6 The electrocatalytic currents of H_2O_2 on the MP-11/cysteamine/Au/GCE in 20 mMN_2 saturated phosphate solution (pH 7.0) at 100 mV · s^{-1}. Curve a-e: 0, 0.039, 0.107, 0.146, and 0.195 mM

(Fig. S2, Supporting Information) and cysteamine/Cu/GCE (Fig. S3, Supporting Information), respectively. As expected, similar observations are obtained on the MP-11/cysteamine/Cu@Au/GCE, except for lower peak currents and smaller k_s (1.70 s^{-1}). However, only the reduction peak of MP-11 is observed on the MP-11/cysteamine/Cu/GCE (Fig. S3, Supporting Information), showing that the immobilized MP-11 partially lost its bioactivity. Thus, the cysteamine coated porous network-like Au film has a larger electroactive surface area and better biocompatibility, which is important for the immobilization of MP-11. The thiols in cysteamine are chemisorbed on the Au surface and the –COOH groups are given for the covalent immobilization of MP-11. Therefore, the functional porous Au film provides a better platform to host the protein and remain its bioactivity.

The pH-dependent interfacial redox process of the immobilized MP-11 was also investigated in a pH range from 3.0 to 9.0 (Fig. 4). With the increase of pH, the reduction and oxidation potentials drop down on the MP-11/cysteamine/Au/GCE (Fig. S4, Supporting Information), suggesting protons are involved in the interfacial redox process [4, 19, 31]. At much lower pH, the carboxyl head-groups from the self-assembled cysteamine are protonated and even denaturated the immobilized protein,

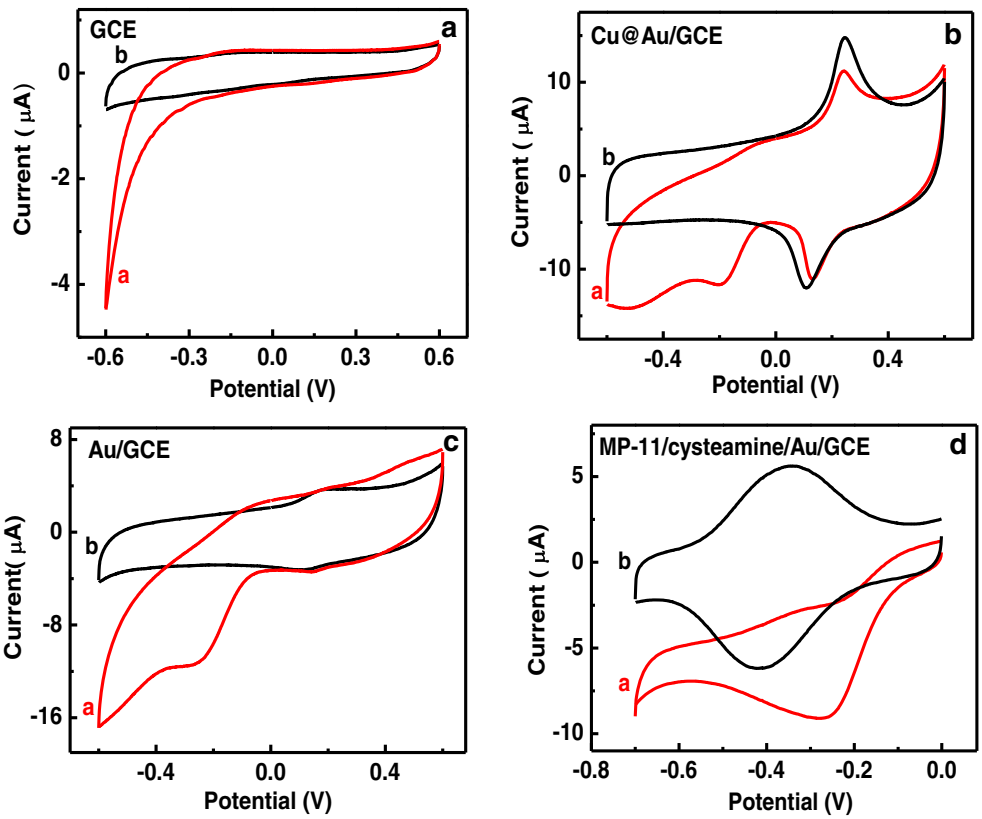

Fig. 5 CVs of the (**a**) bare GCE, (**b**) Cu@Au/GCE, (**c**) Au/GCE, and (**d**) MP-11/cysteamine/Au/GCE in the saturated (red curve **a**) and free (black curve **b**) of O_2 at 100 mV · s^{-1}

resulted in much smaller peak currents [32]. Conversely, with the increase of pH above the isoelectric point, the negative charges on the protein surface would increase, leading to the gradual increase of the coulombic repulsive forces between the charged protein [33]. Therefore, the peak currents reach the maximum values at pH 7.0.

Practical applications

In the past two decades, MP-11 has displayed high electrocatalytic activity towards the reduction of O_2, H_2O_2, and organic peroxides [3], and thus widely used in biofuel cells (or biosensors). In this work, we firstly examined the catalytic ability of the MP-11/cysteamine/Au/GCE towards the reduction of O_2 (Fig. 5). In the presence of O_2, the catalytic currents significantly increase with the decrease of the oxidation peak currents. It reveals that the immobilized protein has high catalytic activity towards the reduction of O_2.

For comparison, control experiments are also performed on the bare GCE, Cu@Au/GCE, and Au/GCE under the same conditions. At bare GCE, the redox currents are almost constant with (Fig. 5a, curve a) and without O_2 (Fig. 5a, curve b). Meanwhile, the onset reduction potential of O_2 is located at −0.3 V, more negative than that on the MP-11/cysteamine/Au/GCE (Fig. 5d). However, on the Cu@Au/GCE, an oxidation peak is emerged at 0.24 V and a reduction peak is located at 0.13 V in the absence of O_2 (Fig. 5b, curve b). These peaks are assigned to the redox of the Cu coexisted with Au. Furthermore, another new reduction peak is emerged at −0.2 V in the presence of O_2, which comes from the reduction of O_2 (Fig. 5b, curve a). After the removal of the template in 2 M HNO_3, the Au/GCE is obtained and the redox peaks of Cu are almost disappeared (Fig. 5c). The Au/GCE exhibits higher catalytic currents towards O_2 at −0.2 V (Fig. 5c, curve a), which is larger than that of the Cu@Au/GCE, because of larger surface of the porous network-like Au film.

More importantly, the catalytic ability of the MP-11/cysteamine/Au/GCE was also investigated using H_2O_2 as another model probe (Fig. 6). Evidently, a pair of reversible redox peaks of MP-11 is emerged without H_2O_2 (Fig. 6, curve a). After successive addition of H_2O_2 into blank phosphate solutions, the catalytic currents are linearly increased with the H_2O_2 concentrations from 10 μM to 16.0 mM. The detection limit of H_2O_2 is 0.4 μM (3 S/N). To evaluate the catalytic performance of the as-prepared H_2O_2 biosensor, other materials and methods were used for comparison (Table S1, Supporting Information). Notably, the performance of the H_2O_2 biosensor is among the best of previous reports, for example, showing lower detection limit and broader linear range, which can be potentially used for the detection of H_2O_2 in real samples.

For comparison, control experiments on the MP-11/cysteamine/Cu@Au/GCE (Fig. S5, Supporting Information) were also investigated, which displayed much smaller catalytic currents under the identical conditions. Surprisingly, after the addition of 0.039 mM H_2O_2, nearly no catalytic current is observed on the MP-11/cysteamine/Cu/GCE (Fig. S6, Supporting Information) under the same conditions. It indicates that the catalytic activity of the immobilized MP-11 is almost lost in this case. These results further supports that the porous network-like Au film is a good candidate to enhance the catalytic efficiency of the immobilized protein.

The selectivity of the MP-11/cysteamine/Au/GCE was investigated by the detection of H_2O_2 with some potential coexisting compounds in biological systems. When the concentrations of these potential interferents such as uric acid, glucose, and ascorbic acid were two or three times higher than that of H_2O_2, nearly no effects can be detected in this system. This is mainly due to the lower detection potential of H_2O_2. Moreover, the stability of the MP-11/cysteamine/Au/GCE was checked within 2 weeks. The catalytic current responses kept approximately 94 % of its initial values when the electrode was stored at 4 °C and measured occasionally.

Conclusions

In this work, porous network-like Au films were obtained with the assistance of the sacrificial template of Cu film. The cysteamine modified Au film was successfully used for the covalent immobilization of MP-11, which can directly transfer electrons with the electrode and shows high electrocatalytic activity towards the reduction of O_2 and H_2O_2, respectively. The porous network-like Au film provides a good platform for the construction of bioelectronics devices such as biosensors and biofuel cells.

Acknowledgments This work was financially supported by the Nation Natural Science foundation of China (20805011, 20905021, 20905055, 51108424, 21175218 and 21275130), the Foundation of the Ministry of Education of China for Returned Scholars (A.J. Wang and J.J. Feng), and the opening funding of State Key Laboratory of Analytical Chemistry for Life Science of Nanjing University (SKLACLS1107 for J.J. Feng).

References

1. Tsou CL (1951) Cytochrome c modified by digestion with proteolytic enzymes. 1. Digestion. Biochem J 49:362
2. Harbury HA, Loach PA (1960) Oxidation-linked proton functions in heme octa- and undecapeptides from mammalian cytochrome c. J Biol Chem 235:3640
3. Yarman A, Nagel T, Gajovic-Eichelmann N, Fischer A, Wollenberger U, Scheller FW (2011) Bioelectrocatalysis by microperoxidase-11 in a multilayer architecture of chitosan embedded gold nanoparticles. Electroanalysis 23:611

4. Zhou Y, Liu S, Jiang H-J, Yang H, Chen H-Y (2010) Direct electrochemistry and bioelectrocatalysis of microperoxidase-11 immobilized on chitosan-graphene nanocomposite. Electroanalysis 22:1323
5. Astuti Y, Topoglidis E, Durrant JR (2011) Use of microperoxidase-11 to functionalize tin dioxide electrodes for the optical and electrochemical sensing of hydrogen peroxide. Anal Chim Acta 686:126
6. Chen S, Yuan R, Chai Y, Hu F (2012) Electrochemical sensing of hydrogen peroxide using metal nanoparticles: a review. Microchim Acta 180:15
7. Abdelwahab AA, Koh WCA, Noh H-B, Shim Y-B (2010) A selective nitric oxide nanocomposite biosensor based on direct electron transfer of microperoxidase: Removal of interferences by co-immobilized enzymes. Biosens Bioelectron 26:1080
8. Wang M, Zhao F, Liu Y, Dong S (2005) Direct electrochemistry of microperoxidase at Pt microelectrodes modified with carbon nanotubes. Biosens Bioelectron 21:159
9. Willner I, Yan YM, Willner B, Tel-Vered R (2009) Integrated enzyme-based biofuel cells–A review. Fuel Cells 9:7
10. Mazzei F, Favero G, Frasconi M, Tata A, Pepi F (2009) Electron-transfer kinetics of microperoxidase-11 covalently immobilised onto the surface of multi-walled carbon nanotubes by reactive landing of mass-selected ions. Chem-Eur J 15:7359
11. Cheung KC, Wong WL, Ma DL, Lai TS, Wong KY (2007) Transition metal complexes as electrocatalysts—Development and applications in electro-oxidation reactions. Coord Chem Rev 251:2367
12. Wu Y, Hu S (2007) Biosensors based on direct electron transfer in redox proteins. Microchim Acta 159:1
13. Pingaron JM, Yáñez-Sedeño P, González-Cortés A (2008) Gold nanoparticle-based electrochemical biosensors. Electrochim Acta 53:5848
14. Zeng S, Yong K-T, Roy I, Dinh X-Q, Yu X, Luan F (2011) A review on functionalized gold nanoparticles for biosensing applications. Plasmonics 6:491
15. Chen Y, Kung S-C, Taggart DK, Halpern AR, Penner RM, Corn RM (2010) Fabricating nanoscale dna patterns with gold nanowires. Anal Chem 82:3365
16. Grzelczak M, Perez-Juste J, Mulvaney P, Liz-Marzan LM (2008) Shape control in gold nanoparticle synthesis. Chem Soc Rev 37:1783
17. Alexandridis P (2011) Gold nanoparticle synthesis, morphology control, and stabilization facilitated by functional polymers. Chem Eng Technol 34:15
18. Kuo S-W, Yang H-Y, Wang C-F, Jeong K-U (2012) Nanoporous gold film prepared by the epoxidation of poly(styrene-b-butadiene) diblock copolymer templated micelles. Macromol Chem Phys 213:344
19. Chen Z, Sun D, Zhou Y, Zhao J, Lu T, Huang X, Cai C, Shen J (2011) Nano polyurethane-assisted ultrasensitive biodetection of H_2O_2 over immobilized microperoxidase-11. Biosens Bioelectron 29:53
20. Song Y-Y, Gao Z-D, Kelly JJ, Xia X-H (2005) Galvanic deposition of nanostructured noble-metal films on silicon. Electrochem Solid-State Lett 8:C148
21. Song YY, Jia WZ, Li Y, Xia XH, Wang QJ, Zhao JW, Yan YD (2007) Synthesis and patterning of prussian blue nanostructures on silicon wafer via galvanic displacement reaction. Adv Funct Mater 17:2808
22. Zhu X, Yuri I, Gan X, Suzuki I, Li G (2007) Electrochemical study of the effect of nano-zinc oxide on microperoxidase and its application to more sensitive hydrogen peroxide biosensor preparation. Biosens Bioelectron 22:1600
23. Zhang X, Wang G, Liu X, Wu H, Fang B (2008) Copper dendrites: synthesis, mechanism discussion, and application in determination of l-tyrosine. Cryst Growth Des 8:1430
24. Huang C-J, Chiu P-H, Wang Y-H, Yang C-F (2006) Synthesis of the gold nanodumbbells by electrochemical method. J Colloid Interface Sci 303:430
25. Li Y, Song Y-Y, Yang C, Xia X-H (2007) Hydrogen bubble dynamic template synthesis of porous gold for nonenzymatic electrochemical detection of glucose. Electrochem Commun 9:981
26. Feng J-J, Li A-Q, Lei Z, Wang A-J (2012) Low-potential synthesis of clean au nanodendrites and their high performance toward ethanol oxidation. ACS Appl Mater Interfaces 4:2570
27. Gao W, Xia X-H, Xu J-J, Chen H-Y (2007) Three-dimensionally ordered macroporous gold structure as an efficient matrix for solid-state electrochemiluminescence of $Ru(bpy)_3^{2+}$/TPA system with high sensitivity. J Phys Chem C 111:12213
28. Zhang L, Zhang J, Zhang C (2009) Electrochemical synthesis of polyaniline nano-network on alpha-alanine functionalized glassy carbon electrode and its application for the direct electrochemistry of horse heart cytochrome c. Biosens Bioelectron 24:2085
29. Xie Y, Hu N, Liu H (2009) Bioelectrocatalytic reactivity of myoglobin in layer-by-layer films assembled with triblock copolymer Pluronic F127. J Electroanal Chem 630:63
30. Zhao Y-D, Bi Y-H, Zhang W-D, Luo Q-M (2005) The interface behavior of hemoglobin at carbon nanotube and the detection for H_2O_2. Talanta 65:489
31. Jin B, Wang G-X, Millo D, Hildebrandt P, Xia X-H (2012) Electric-field control of the pH-dependent redox process of cytochrome c immobilized on a gold electrode. J Phys Chem C 116:13038
32. Kafi AKM, Wu G, Chen A (2008) A novel hydrogen peroxide biosensor based on the immobilization of horseradish peroxidase onto Au-modified titanium dioxide nanotube arrays. Biosens Bioelectron 24:566
33. Wang CH, Yang C, Song YY, Gao W, Xia XH (2005) Adsorption and direct electron transfer from hemoglobin into a three-dimensionally ordered macroporous gold film. Adv Funct Mater 15:1267